

Diffusion measurements in oriented phospholipid bilayers by $^1\text{H-NMR}$ in a static fringe field gradient

Paul Karakatsanis

Physik Department E22, Technische Universität München, D-85748 Garching, Germany

Thomas M. Bayerl

Physikalisches Institut EP-V, Universität Würzburg, D-97047 Würzburg, Germany

(Received 29 February 1996)

For the first time, to our knowledge, self-diffusion of lipids and water in lipid bilayers is studied by proton NMR measurements in the fringe field of a superconducting magnet. Highly oriented multilayer stacks of dipalmitoyl phosphatidylcholine were used, and the lateral diffusion coefficient of the lipid D_L was measured at different temperatures and water contents of the sample. Additionally, the lateral diffusion coefficient D_W of the water between the lipid bilayers was determined. The results demonstrate that our technique is extremely well suited for a precise determination of diffusion coefficients in oriented membranes, and that it allows the simultaneous measurement of both lipid and water diffusion. The values of D_L and D_W obtained by this technique agree well with published data obtained by other NMR techniques and by fluorescence methods. A comparison of our data with those obtained in a previous study by quasielastic neutron scattering provides information about the contribution of short- and long-range diffusion to the measured diffusion coefficient due to the intrinsic length and time scale of the experiments. [S1063-651X(96)00508-9]

PACS number(s): 87.22.Bt, 07.57.Pt, 66.10.Cb, 76.60.-k

I. INTRODUCTION

The best established dynamical phenomenon in model membranes is the lateral diffusion of the lipid constituents along the membrane plane. It has been studied by fluorescence recovery after photobleaching (FRAP) [1–3], excimer techniques [4,5], electron spin resonance [6], various NMR techniques [7–11], and quasielastic neutron scattering (QENS) [12,13]. The lateral diffusion coefficients D_L of lipids determined by these methods differ by up to two orders of magnitude. Besides the different experimental errors, the origin of these differences is most likely that some methods are sensitive only to long-range diffusion (e.g., FRAP), while others (QENS) pick up contributions from extremely short-range diffusion processes [14]. Similar considerations apply to the measurement of water diffusion in membranes.

A severe shortcoming of some of the above techniques is their reliance on labels; i.e., the diffusion coefficient measured is that of the labeled molecule and not that of the bulk molecules in the bilayer. Taking into account that the labels are often rather bulky groups (e.g., spin labels or fluorescence dyes), which can be expected to modulate the interaction of the lipid with the surrounding molecules, a discrepancy between the measured D_L values and the bulk lipid diffusion is quite likely. This problem is even more serious for techniques involving bimolecular reactions (e.g., excimer methods) where phase separations due to the presence of pyrene labeled probes in the membrane cannot be excluded.

QENS and NMR are the only methods, which—in general—do not require any particular labeling. However, the application of QENS is restricted due to large substance requirements (typically 0.5–1 g of lipid per sample) and limited neutron beamtime. Thus NMR remains as the only potentially label free method to study lateral diffusion in lipid bilayers. The classical NMR method for measuring lateral diffusion is the pulsed field gradient method (PFG) which

requires a specially equipped spectrometer. The experimental error (particularly for measuring diffusion in highly viscous environments like membranes) is largely determined by the switching time of the gradients.

Some of these drawbacks can be overcome by the recently introduced technique of measuring diffusion by NMR in the fringe of superconducting magnets. This technique will be referred to in the following as the supercon fringe field (SFF) technique. SFF provides strong and extremely stable magnetic field gradients, and elegantly bypasses the problem of switching gradients on and off. Therefore a previously unreachable experimental accuracy can be expected in the study of membrane system dynamics despite short transverse relaxation times and low diffusion constants.

So far, the SFF technique has not been applied to the study of diffusion in membranes. It requires well-oriented stacks of membranes and an optimum of sample space filling in order to exploit its potential advantages in accuracy. Here we present data on lateral diffusion of lipid and water obtained by this technique on highly oriented stacks of DPPC multilayers. Finally, these very accurate measurements provide support for the validity of the free volume model of lateral diffusion in membranes, and demonstrate that a detailed NMR study of lateral diffusion in such systems is possible without a dedicated pulsed field gradient spectrometer.

II. MATERIALS AND METHODS

A. Materials

1,2-dipalmitoyl-*d*62-sn-glycero-3-phosphocholine (DPPC-*d*₆₂) and 1,2-dipalmitoyl-*d*62-sn-glycero-3-phosphocholine-1,1,2,2-*d*4-*N,N,N*-trimethyl-*d*9 (DPPC-*d*₇₅) were obtained from Avanti Polar Lipids Inc. (Alabaster, AL, U.S.A.). All organic solvents were HPLC quality from Fluka (Buchs, Switzerland). Purified $^2\text{H}_2\text{O}$ was obtained from Deuchem GmbH (Leipzig, Germany); the H_2O was from a laboratory

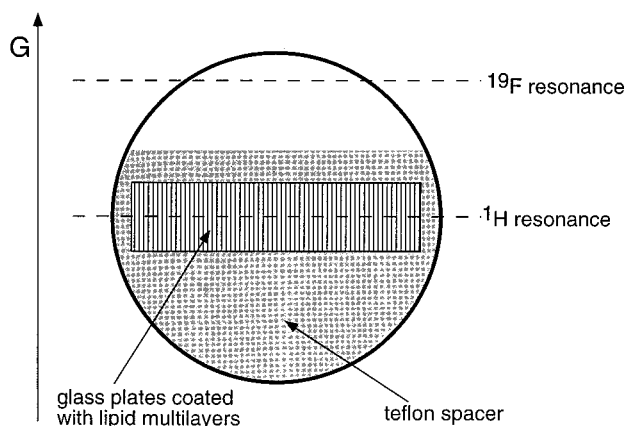


FIG. 1. Schematic depiction of the cross section of a lipid sample in a glass tube with 10-mm outer diameter. 70 stacked glass plates were used as substrates, each of them carrying about 1500 bilayers. The positions of the ^1H and ^{19}F resonances, which have about 100- μm thickness, are indicated by dashed lines.

water ultrapurification system (Millipore GmbH, Eschborn, Germany). Thin glass plates of 60- μm thickness were purchased from Paul Marienfeld GmbH & Co. KG (Bad Merzheim, Germany).

B. Methods

1. Sample preparation

Oriented phospholipid bilayers were prepared as described in [13], using 60- μm thin glass plates as substrate. Figure 1 shows schematically the sample geometry. A sample consists of about 70 stacked glass plates, $2 \times 12.5 \text{ mm}^2$ each, with a total amount of 30-mg lipid.

All samples were dried in a vacuum overnight at room temperature and then rehydrated with $^2\text{H}_2\text{O}$ or $^1\text{H}_2\text{O}$, depending on whether water or lipid diffusion was to be measured. Finally the stack of glass plates was placed in a 10-mm glass tube and sealed with Teflon caps and Viton o-rings.

2. Sample characterization

All samples were characterized with respect to hydration and orientation by ^2H broadline NMR measurements in the homogeneous field of the magnet. The $^2\text{H}_2\text{O}$ /lipid molar ratio of the sample was determined by integrating the spectrum at the $\theta=90^\circ$ orientation, i.e., the membrane normal perpendicular to the magnetic field B_0 [see Fig. 2(a)]. The bound $^2\text{H}_2\text{O}$ and the deuterated DPPC- d_{62} terminal methyl groups give sharp, well separated peaks, allowing a precise determination of their integrals. The hydration of $\text{H}_2\text{O}/\text{DPPC-}d_{75}$ -samples was determined gravimetrically. The relative error in the determination of the hydration was less than 10%.

The quality of orientation was examined by acquiring a spectrum in the L_α phase at the magic angle [Fig. 2(b)], where all quadrupole splittings vanish in the case of perfect orientation. The width of the remaining central peak gives a mosaic spread of typically better than 5° . This includes orientation errors both on a macroscopic scale, such as distortions in the orientation of the glass plates and in the accuracy of the goniometer, and on a microscopic scale, like undula-

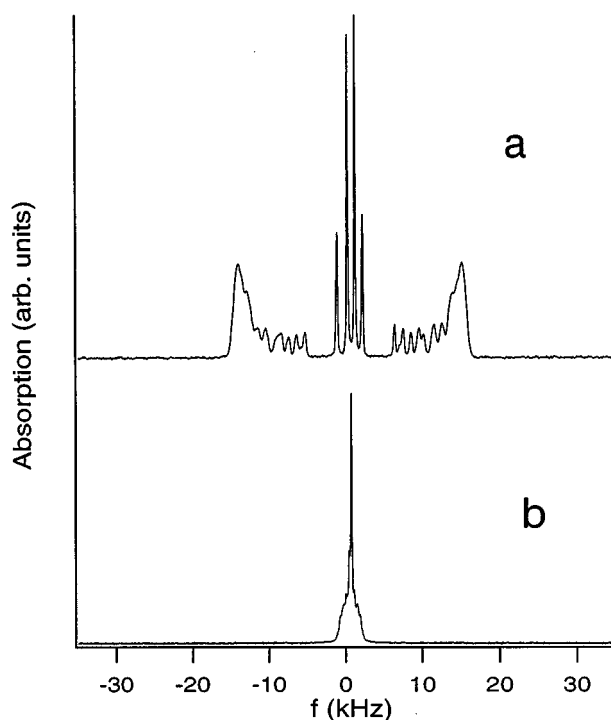


FIG. 2. (a) ^2H -NMR spectrum of a DPPC- d_{62} lipid sample, hydrated with $^2\text{H}_2\text{O}$ ($n_w=6$), in the fluid L_α phase at $\theta=90^\circ$. (b) The same sample as (a), but at the magic angle $\theta=54.7^\circ$. The width of the remaining peak is 4.6 kHz, which gives a mosaic spread of 3° .

tions and collective director fluctuations.

The nonoriented fraction of the sample shows up in a broad signal, hardly visible to the eye, in the frequency range of a DPPC- d_{62} powder spectrum in the L_α phase. By comparing the integrals of nonoriented and oriented fractions, the former can be estimated. If not indicated otherwise, our samples had less than 7% nonoriented fraction.

3. NMR hardware

All NMR experiments were performed at a 400-MHz NMR spectrometer (VARIAN VXR 400), equipped with a VARIAN wide-line high-power probe and a 10-mm six turn-coil. The 90° pulse length for the ^1H resonance in the fringe field was about 2.5 μs .

For diffusion measurements the probe was placed in the fringe field, 22 cm below its usual position in the homogeneous field, corresponding to a ^1H resonance frequency of 214 MHz and a magnetic field gradient of $G=58 \text{ T/m} \pm 2\%$ at the sample site. The gradient was calibrated with self-diffusion measurements of pure $^1\text{H}_2\text{O}$ (see Fig. 3), using the tabulated values of $D_{\text{H}_2\text{O}}$ in [15]. The error is mainly due to the temperature stability of the probe ($\pm 0.5 \text{ K}$).

Great care was taken to adjust the sample position properly to avoid any signal arising from the ^{19}F resonance, which is situated just 4 mm above the ^1H resonance for our setup. Signals from tube sealings were avoided by using sufficiently long sample tubes. Note that not the whole sample, but only a thin slice of about 100- μm thickness, is excited in the SFF experiment owing to the strong magnetic field gra-

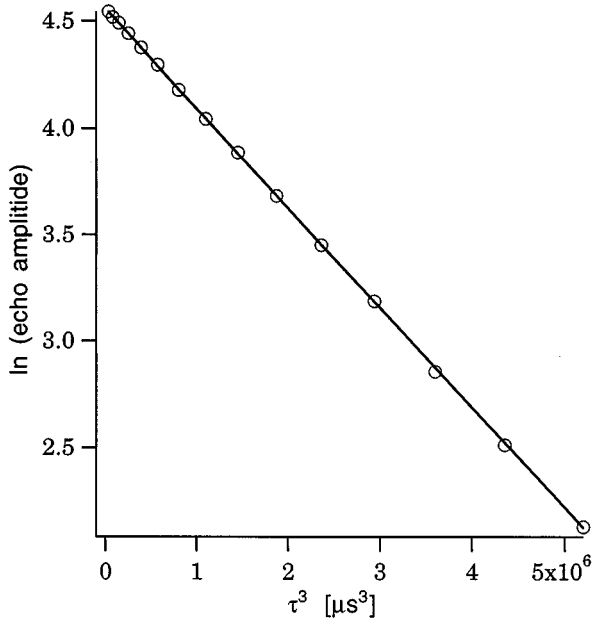


FIG. 3. Gradient calibration with a pure water sample at 35 °C. A Hahn spin-echo sequence was used with pulse delays varying from $\tau=33$ to 170 μs . Error bars are smaller than the symbols in this plot. The slope of the plot is $-\frac{2}{3}\gamma^2 G^2 D$, giving a magnetic field gradient of $G=58$ T/m \pm 2%.

dients and the limited rf bandwidth. However, it is important that this slice is large compared to the characteristic length scale $q^{-1}=\gamma G\tau_1$ (see Sec. IV), which is on the order of 1 μm , to maintain the validity of Eqs. (2) and (4). With this setup and using a typical lipid sample, the signal to noise ratio is about $S/N=3$ per transient.

4. NMR methods

All diffusion measurements were performed by ^1H -NMR at a fixed position in the fringe field. Diffusion of pure $^1\text{H}_2\text{O}$ was measured with a Hahn spin-echo sequence

$$90^\circ_x - \tau - 180^\circ_y - \tau - (\text{echo}). \quad (1)$$

The amplitude A_{se} of the spin echo in the case of normal diffusion and in the presence of a constant field gradient G is [16]

$$A_{\text{se}}=A_0 e^{-2\pi/T_2} e^{-(2/3)\gamma^2 G^2 D \tau^3}. \quad (2)$$

D is the diffusion coefficient of the sample, and γ is the gyromagnetic ratio of the nucleus. The first exponential term, describing the transverse relaxation (T_2), is negligible for a pure water sample.

However, for short T_2 and $T_2 \ll T_1$ (longitudinal relaxation), which is typical for dipolar relaxation in the slow correlation time limit, diffusion measurements are no longer feasible with the Hahn echo sequence. Therefore diffusion in lipid samples was measured with a stimulated echo sequence

$$90^\circ_y - \tau_1 - 90^\circ_y - \tau_2 - 90^\circ_y - \tau_1 - (\text{echo}). \quad (3)$$

The amplitude A_{st} of the stimulated echo is [17–22]

$$A_{\text{st}}=\frac{1}{2}A_0 e^{-2\tau_1/T_2} e^{-\tau_2/T_1} e^{-\gamma^2 G^2 D \tau_1^2 [(2/3)\tau_1 + \tau_2]}. \quad (4)$$

A major advantage of the stimulated echo in the case of $T_2 \ll T_1$ is that it allows diffusion encoding during the τ_2 interval, while the magnetization is stored along the z axis and relaxation is solely determined by T_1 processes [18]. In order to consider T_2 and T_1 relaxation explicitly, diffusion measurements were performed as follows.

First, τ_1 was kept fixed and an array of τ_2 's was chosen. Fitting the resulting decay of the echo amplitudes with a single exponential gives the decay constant $s(\tau_1)$. Then the procedure was repeated for different τ_1 values. Finally, $s(\tau_1)$ was plotted against τ_1^2 . The resulting slope of this plot is $\gamma^2 G^2 D$.

The τ_1 values were in the range of 20–80 μs . Appropriate τ_2 values were chosen to give a reasonable echo decay (see Figs. 4 and 7). 300 transients were acquired for each echo amplitude, with a repetition time of 2 s. A multislicing technique as proposed in [20] was used, and allowed an improvement of the signal to noise ratio by a factor of about 2.

5. Error estimation

Possible errors in the determination of diffusion coefficients with the SFF method may arise from the gradient calibration (2%), the statistical noise (here about 3%), and from the nonoriented fraction p of the sample. To estimate the latter, we assumed the defects to be of spherical geometry and diameter larger than the typical length scale of the experiment. In the limit of small τ values one can evaluate the multiexponential decay and obtain an averaged $D_{\text{sph}}=2/3 D_0$ for the spheres. So the measured D is reduced systematically to $D=D_0(1-1/3p)$ for the 90° position, and increased to $2/3 p D_0$ for the 0° position.

Thus the absolute value of D can be determined with an accuracy better than 10%, while relative changes of D in the same sample, caused, e.g., by temperature changes, can be observed with only a 3% standard deviation.

III. EXPERIMENTAL RESULTS

A. Lipid diffusion in oriented membranes

Lipid diffusion of oriented DPPC- d_{62} - $^2\text{H}_2\text{O}$ multilayers in the fluid L_α phase was measured at two different hydrations, and as a function of temperature and orientation of the membrane normal to the magnetic field gradient. Figure 4 shows typical raw data and analysis of this system for a temperature of 57 °C and a $^2\text{H}_2\text{O}$ /lipid molar ratio $n_w=6$. All data are in excellent agreement with the theoretical predicted $e^{-\tau_1 \tau_2^2}$ dependence of the stimulated echo amplitude, which is characteristic for diffusional processes. The error bars shown in Fig. 4 represent the single standard deviation of the baseline noise or of the respective fits. The linear fit of slopes vs τ_1^2 in Fig. 4(b) gives a lipid diffusion coefficient of $D_L=1.02 \times 10^{-11}$ m 2 /s with a standard deviation of $\pm 3\%$.

1. Temperature and hydration dependence

Figure 5 shows the temperature dependence of D for a fully hydrated lipid sample ($n_w=15$). The Arrhenius representation was chosen for the determination of an apparent activation energy E_a that allows comparison with previous

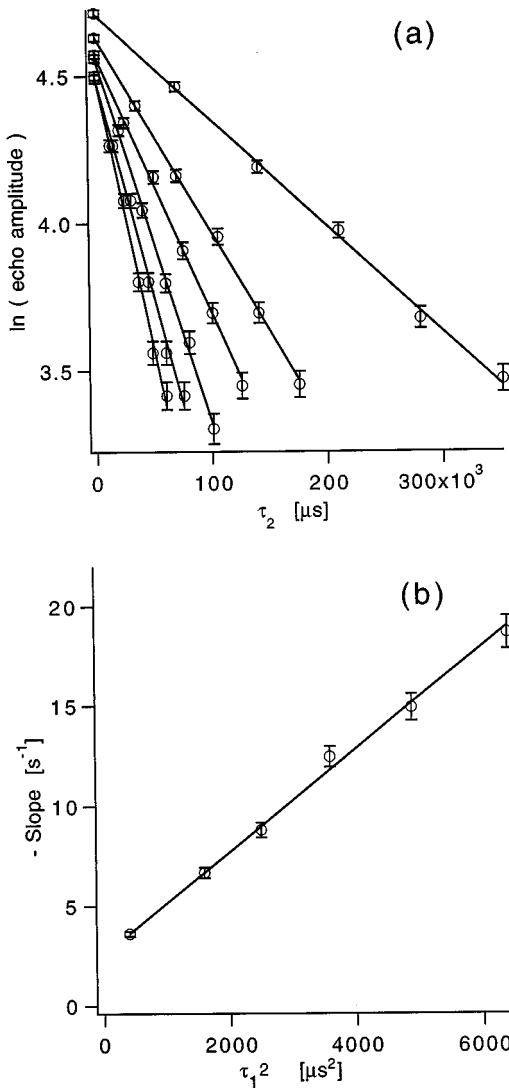


FIG. 4. Lipid diffusion in oriented DPPC- $d_{62}/^2\text{H}_2\text{O}$, at $n_w=6$ and $T=57^\circ\text{C}$. (a) Echo amplitudes of the stimulated echo experiment as a function of the mixing time τ_2 for different values of $\tau_1=20, 40, 50, 60, 70,$ and $80 \mu\text{s}$ starting with the lowest slope. The solid lines represent linear fits to the data. (b) Plot of the slope of the fits from (a) vs τ_1^2 . The slope of this linear fit (solid line) is $\gamma^2 G^2 D$, giving $D_L=1.02 \times 10^{-11} \text{ m}^2/\text{s}$, with a standard deviation of $\pm 3\%$.

measurements of D_L by other methods. We obtain $E_a=35 \text{ kJ/mol} \pm 10\%$ for this plot. Humidity was kept constant over the measurement by inserting a sponge soaked with $^2\text{H}_2\text{O}$ in the sample tube.

Besides the fully hydrated sample, D_L was also determined for a sample with $n_w=6$. We obtained a value of $D_L=1.02 \times 10^{-11} \text{ m}^2/\text{s}$, i.e., half the value we measured at full hydration.

2. Orientation dependence

The SFF method combined with the use of oriented membrane samples offers a unique opportunity to test the theoretical expectation for diffusion in such a system. Therefore D_L was measured at four different angles of the membrane normal to the magnetic field gradient. The results are shown

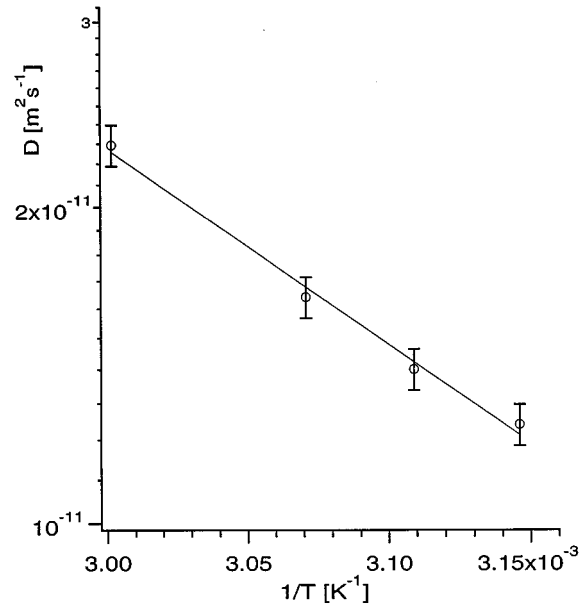


FIG. 5. Arrhenius plot of the lipid diffusion coefficient D_L of a DPPC- $d_{62}/^2\text{H}_2\text{O}$ sample at high hydration ($n_w=15$). The temperature range was $45\text{--}60^\circ\text{C}$ (all fluid phase).

in Fig. 6. Note that the error increases with decreasing angle due to the corresponding reduction of the amount of lipid in the excited sample slice. For the 0° orientation a sample with different geometry had to be used, consisting of four stacked glass plates, $12 \times 8 \text{ mm}^2$ in size, each coated with about 1500 bilayers. The nonoriented fraction of this sample was 20%.

The data in Fig. 6 demonstrate clearly the anisotropy of the lipid diffusion in membranes. Geometrical considerations lead to a $D_L \sim \sin^2 \theta$ dependence, which is indicated by the

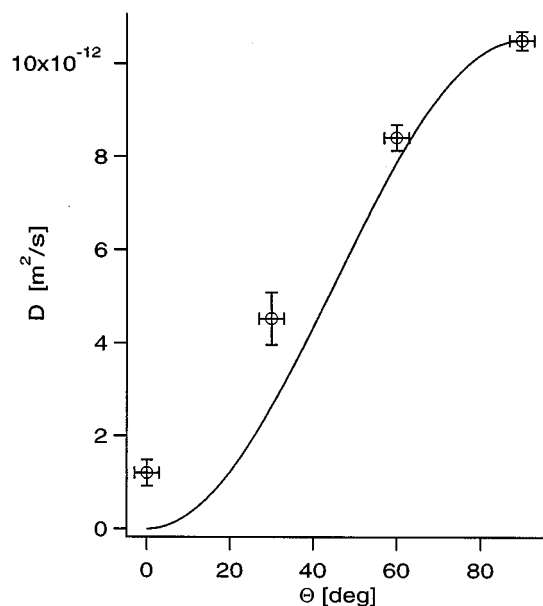


FIG. 6. Orientation dependence of D_L for the same sample as in Fig. 4. θ is the angle between membrane-normal and magnetic field gradients.

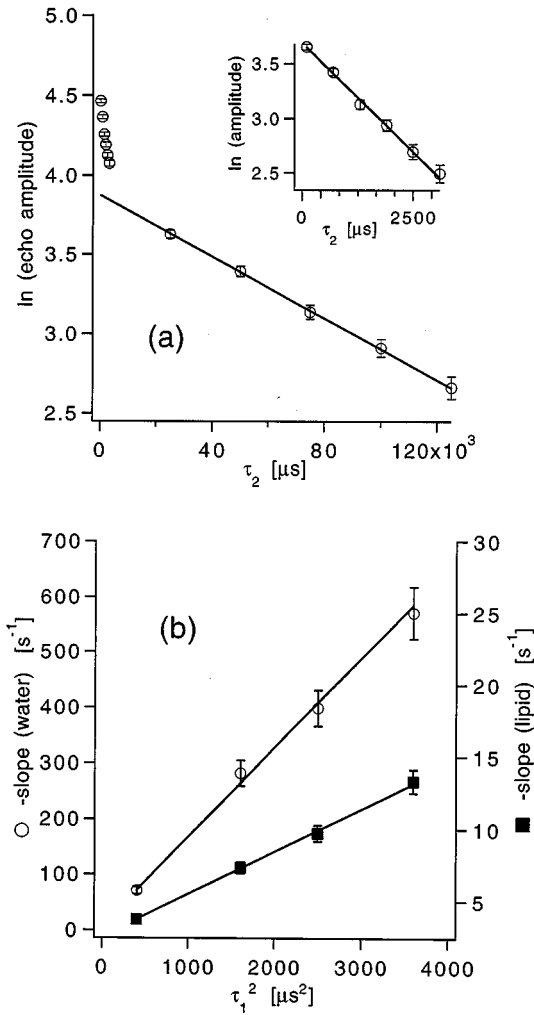


FIG. 7. Simultaneous measurement of D_L and D_W on an oriented DPPC- d_{75} / $^1\text{H}_2\text{O}$ sample at $n_w=10$ and $T=53$ °C. The echo amplitudes of the stimulated echo experiment for $\tau_1=50$ μs are shown in (a). The fast decay for short τ_2 values is due to the bound water, and the slow decay arises from the remaining lipid protons. The inset in (a) shows the amplitudes of the water signal after subtraction of the lipid-background signal. (b) Plot of the slope of the fits from (a) vs τ_1^2 for the lipid decay (solid squares) and water decay (open circles). Linear fits to these data give $D_W=66.8 \times 10^{-11}$ $\text{m}^2/\text{s} \pm 6\%$ and $D_L=1.22 \times 10^{-11}$ $\text{m}^2/\text{s} \pm 6\%$.

full line in Fig. 6. Our experimental D_L values deviate from this line mainly for low θ . This behavior can be explained by the increasing influence of the nonoriented lipid fraction at low θ , and by the high statistical error in this region.

B. Simultaneous measurements of lipid and water diffusion

Measurement of the water diffusion was achieved by substituting $^2\text{H}_2\text{O}$ with $^1\text{H}_2\text{O}$ and DPPC- d_{62} by the nearly full deuterated DPPC- d_{75} . The hydration of this sample was $n_w=10 \pm 1$.

Figure 7 shows the stimulated echo amplitude vs the mixing time τ_2 for $\tau_1=50$ μs . This decay is clearly biexponential with the water dominating the steep initial part, while the glycerol protons of the DPPC- d_{75} account for the flat decay

of long τ_2 . This separation of the decay times, caused by the faster T_1 relaxation and diffusion of the water component compared to the lipids, is sufficiently large for all the τ_1 values to perform a reliable biexponential fit.

As can be seen from the insert in Fig. 7(a), both the initial and the final decays can be approximated very well by a single exponential. This allows a simultaneous determination of water (D_W) and lipid (D_L) diffusion constants from a single experiment.

At a temperature of 53 °C we obtained $D_W=66.8 \times 10^{-11}$ $\text{m}^2/\text{s} \pm 6\%$ and $D_L=1.22 \times 10^{-11}$ $\text{m}^2/\text{s} \pm 6\%$. A second measurement was performed at 30 °C where DPPC- d_{75} is in the gel phase state. Under this conditions, lipid long-range lateral diffusion becomes unmeasurably small ($D_L < 0.06 \times 10^{-11}$ m^2/s) for the SFF method, while water diffusion remains rather undisturbed ($D_W=44.0 \times 10^{-11}$ $\text{m}^2/\text{s} \pm 6\%$).

IV. DISCUSSION

The above results demonstrate that the SFF technique can be used for an accurate determination of diffusion coefficients in phospholipid bilayers at different hydrations and temperatures. Moreover, it allows us to measure D for both the phospholipid and the surrounding water simultaneously in one experiment. This is a clear advantage over techniques like FRAP, which rely on the use of dye labeled lipid molecules. In order to compare the D values obtained by SFF with those determined by other techniques, a consideration about the characteristic length scale l_{SFF} , i.e., the characteristic distance over which root-mean-square molecular displacements are sampled, is required.

As one can see from [23,17], the echo amplitude of the stimulated echo experiment $A_{\text{st}}(q, \tau_2)$, with the momentum q defined as $q = \gamma G \tau_1$, is in complete analogy with the incoherent, intermediate scattering function $I_{\text{inc}}(q, t)$ in quasi-elastic neutron scattering. In our set of parameters q was varied from $(3.2 \mu\text{m})^{-1}$ to $(0.8 \mu\text{m})^{-1}$. The τ_2 decays of lower q values are dominated by T_1 relaxation, these with higher q values are dominated by diffusion, so that the sensitive length scale for diffusion measurements is in the order of 1 μm . Hence l_{SFF} is roughly one order of magnitude below that of FRAP [1] measurements, but three orders of magnitude larger than that of the QENS [13,24] technique. Among other NMR methods, the length scale of the two-dimensional ^2H -NMR as well as the PFG technique [8,9] are both in the region of 200–500 nm, while the length scale of the Carr-Purcell-Meiboom-Gill (CPMG) technique for measuring D_L on spherically curved bilayers [10] is in the range of 100 nm.

Using QENS, we previously obtained a value of $D_L=0.97 \times 10^{-11}$ m^2/s for DPPC oriented multilayers at 60 °C and full hydration [13]. This value was obtained by considering separately both long-range diffusion (over distances ≥ 1 nm) and short-range back and forth jumps of the molecules (local diffusion) in a simultaneous fitting model, as both contribute to the QENS line broadening. Without any distinction between local and long-range diffusion, QENS gives a higher value of D_L by nearly two orders of magnitude.

At a length scale closer to the SFF method, FRAP measurements gave $D_L=1.7 \times 10^{-11}$ m^2/s [1], and PFG measure-

ments are reported in the literature with $D_L = 1.9 \times 10^{-11} \text{ m}^2/\text{s}$ [9] (at both 60 °C and full hydration). These values compare favorably with our SFF method, giving $D_L = 2.3 \times 10^{-11} \text{ m}^2/\text{s}$ at 57°, and similar hydration. No data are available for D_L of DPPC measured with the CPMG technique. For POPC, we determined D_L with this technique under hydration similar to $D_L = 0.7\text{--}0.8 \times 10^{-11} \text{ m}^2/\text{s}$ at 50 °C, which seems rather similar to the DPPC values, taking into account the 10° lower temperature for the POPC data.

Similar differences between QENS and SFF also remain for water diffusion measurements. At 30 °C and $n_w = 10$, we obtained $D_w = 44 \times 10^{-11} \text{ m}^2/\text{s}$, while QENS gave roughly a 2.5 times higher value of $D_w = 110 \times 10^{-11} \text{ m}^2/\text{s}$ [24] in terms of a jump diffusion model with a mean residence time of 2.5 ps. To appreciate this discrepancy, one has to consider that the length scale of QENS is less than 10 Å, while the diameter of the water molecule is 3–4 Å. Thus the jump of a water molecule from a DPPC headgroup binding site to the bulk and back (e.g., as caused by the breaking and recreation of hydrogen bonds) will contribute significantly to the QENS result for D_w but certainly not to the SFF result. Moreover, rotational diffusion of the choline headgroup, which persists in the gel phase, will contribute to the local diffusion of the water fraction that is hydrogen bonded to this group over distances ≤ 10 Å for QENS only. The apparent activation energy of the lipid diffusion $E_a = 35 \text{ KJ/mol}$ determined by SFF at full hydration is very similar to the value we measured previously for the fast uniaxial rotation of the water molecules as well as for the slow reorientation of this axis, which both gave $E_a = 32 \text{ KJ/mol}$ at $n_w = 4$ [24]. This suggests that reorientation of water bound to lipid headgroups and the diffusional jump of a lipid molecule are tightly coupled processes. The SFF value for E_a of DPPC is similar to those determined by FRAP ($29 \pm 5 \text{ KJ/mol}$) [1] and by two-dimensional $^2\text{H-NMR}$ ($28 \pm 7 \text{ KJ/mol}$) [25], while excimer ($E_a = 59 \text{ KJ/mol}$) [3] and early PFG studies ($E_a = 69 \text{ KJ/mol}$) [9] provided E_a values almost twice as high for lipids. How-

ever, in considering extraordinarily high values there, it should be noted that the excimer value was determined for monolayers, and that the PFG result might be affected by sample morphology and differences in hydration.

The measurement of D_L at two hydrations gives us the opportunity to check the consistency of our data with the predictions of the free volume model of lateral diffusion [1,4], which describes D_L by the following exponential dependence:

$$\ln(D_L) = \ln(kT/f) - \gamma A^*/(A_{\text{mol}} - A_{\text{cage}}). \quad (5)$$

Here f is the frictional coefficient characterizing the viscous drag of adjacent bilayers on the diffusing lipid. Both internal friction within the bilayer and the friction exerted by adjacent bilayers contribute to f . ($A_{\text{cage}} - A_{\text{mol}}$) is the free area per molecule, A_{cage} is the area of the total solvent cage the lipid can diffuse in, and A^* is the critical free area. The latter is defined as the minimum value of the free area required for diffusional jumps of the test molecule. γ is a geometrical factor that can vary between 0.5 and 1, and accounts for the overlap between free volumes. Connecting our values for D at two hydrations in a double logarithmic representation of $\ln(D)$ vs $1/(A_{\text{cage}} - A_{\text{mol}})$, using the hydration dependent values of $(A_{\text{cage}} - A_{\text{mol}})$ [26,13] gives $\gamma A^* = 15 \text{ \AA}$ and $kT/f = 4.2 \times 10^{-11} \text{ m}^2/\text{s}$. From the latter, a friction coefficient $f = 1.1 \times 10^{-7} \text{ erg s/cm}^2$ is obtained. Assuming that f is dominated by the lipid headgroup–water interaction, the water viscosity can be estimated according to [1] as $\eta = f/(4\pi R)$, where R is the radius of the headgroup. With $R \approx 4 \text{ \AA}$, we obtain $\eta \approx 20 \text{ cp}$, which is more than one order of magnitude higher than the value for free water. It is now interesting to note that our previous QENS measurements [13] gave $kT/f = 4.1 \times 10^{-10} \text{ m}^2/\text{s}$, and thus $\eta \approx 2 \text{ cp}$, while the value of $\gamma A^* = 17.57 \text{ \AA}^2$ compares well with our result. This indicates that the values of f and η depend on the length scale of the diffusion process under consideration, while the critical free area γA^* is largely independent of it.

-
- [1] W. Vaz, R. Clegg, and D. Hallmann, *Biochemistry* **24**, 781 (1985).
- [2] J. Rubenstein, B. Smith, and H. M. McConnell, *Proc. Natl. Acad. Sci. U.S.A.* **76**, 15 (1979).
- [3] R. Merkel, E. Sackmann, and E. Evans, *J. Phys. (Paris)* **50**, 1535 (1989).
- [4] H. Galla, W. Hartmann, U. Theilen, and E. Sackmann, *J. Membrane Biol.* **48**, 215 (1979).
- [5] R. Merkel and E. Sackmann, *J. Phys. Chem.* **98**, 4428 (1994).
- [6] P. Devaux and H. McConnell, *J. Am. Chem. Soc.* **94**, 4475 (1972).
- [7] M. Bloom *et al.*, *Biochemistry* **17**, 5750 (1978).
- [8] G. Lindblom, L. Johansson, and G. Arvidson, *Biochemistry* **20**, 2204 (1981).
- [9] A. Kuo and C. Wade, *Biochemistry* **18**, 2300 (1979).
- [10] T. Köchy and T. Bayerl, *Phys. Rev. E* **47**, 2109 (1993).
- [11] C. Dolainsky, M. Unger, M. Bloom, and T. Bayerl, *Phys. Rev. E* **51**, 4743 (1995).
- [12] J. Tabony and B. Perly, *Biochim. Biophys. Acta* **1063**, 67 (1990).
- [13] S. König *et al.*, *J. Phys. (France) II* **2**, 1589 (1992).
- [14] W. Vaz and P. Almeida, *Biophys. J.* **60**, 1553 (1991).
- [15] R. Mills, *J. Phys. Chem.* **77**, 685 (1973).
- [16] E. Hahn, *Phys. Rev.* **80**, 580 (1950).
- [17] J. Kärgler, H. Pfeifer, and G. Voita, *Phys. Rev. A* **37**, 4514 (1988).
- [18] R. Kimmich, W. Unrath, G. Schnur, and E. Rommel, *J. Magn. Res.* **91**, 136 (1991).
- [19] F. Klammler and R. Kimmich, *Croat. Chem. Acta* **65**, 455 (1992).
- [20] R. Kimmich and E. Fischer, *J. Magn. Res.* **106**, 229 (1994).
- [21] T. Norwodd, *J. Magn. Res.* **103**, 258 (1993).
- [22] D. Demco, A. Johansson, and J. Tegenfeldt, *J. Magn. Res.* **110**, 183 (1994).
- [23] P. Callaghan and A. Coy, *J. Chem. Phys.* **97**, 651 (1992).
- [24] S. König *et al.*, *J. Chem. Phys.* **100**, 3307 (1994).
- [25] C. Dolainsky, P. Karakatsanis, and T. Bayerl (unpublished).
- [26] L. Lis, M. McAlister, N. Fuller, and R. Rand, *Biophys. J.* **37**, 657 (1982).